Histol Histopathol (2016) 31: 897-909

http://www.hh.um.es

Histology and Histopathology

From Cell Biology to Tissue Engineering

Iodine deficiency induces a VEGF-dependent microvascular response in salivary glands and in the stomach

Jessica Vanderstraeten[1], Hanane Derradji[2], Julie Craps[1], Pierre Sonveaux[3], Ides M. Colin[4], Marie-Christine Many[1] and Anne-Catherine Gérard[1]*

[1]Pole of Experimental Morphology, Institute of Experimental and Clinical Research (IREC), Catholic University of Louvain (UCL), Brussels, [2]Radiobiology Unit, Belgian Nuclear Research Centre (SCK-CEN), Mol, [3]Pole of Pharmacology and Therapeutics, Institute of Experimental and Clinical Research (IREC), Catholic University of Louvain (UCL), Brussels and [4]Department of Endocrinology and Diabetology, Regional Hospital Center (CHR) Mons-Hainaut, Belgium

*Present address: Department of Endocrinology and Diabetology, Regional Hospital Center (CHR) Mons-Hainaut, Belgium and Institute of life sciences (ISV), Catholic University of Louvain (UCL), Belgium

Summary. Despite efforts to optimize iodine supply in iodine deficient countries, iodine deficiency (ID) remains a global problem worldwide. Activation of the local microvasculature by ID in the thyroid gland aims at improving the local supply of iodide. For this purpose, the thyrocytes secrete vascular endothelial growth factor (VEGF) that acts on adjacent capillaries, via a reactive oxygen species (ROS)/Hypoxia Inducible factor (HIF)-dependent pathway. Beside the thyroid, other organs including salivary glands and the stomach do express the sodium/iodide symporter (NIS) and are able to take iodide up, potentially rendering them sensitive to ID. To verify this hypothesis, ID-induced effects on the local microvasculature were studied in salivary glands and in the stomach. ID was induced by feeding young mice with an iodide-deficient diet and NIS inhibitor perchlorate in the drinking water. In salivary glands, ID induced a transient increase in HIF-1α protein expression accompanied by a transient, VEGF-dependent increase in blood flow. In the gastric mucosa, ID transiently increased VEGF expression in the mucin-secreting epithelium and in ghrelin-secreting endocrine cells. These observations suggest that microvascular changes in response to ID occur in NIS-expressing tissues other than the thyroid. NIS expressing cells could be viewed as iodide sensors that respond to ID by inducing vascular changes, probably to optimize iodide bioavailability at regional or systemic levels.

Key words: Iodine deficiency, Salivary glands, Stomach, Microvasculature, VEGF

Introduction

Despite ongoing dietary efforts to improve iodine supply, almost 2 billion people still suffer from mild to moderate ID worldwide (Andersson and Zimmermann, 2012; Pearce et al., 2013; WHO, 2015). In order to face iodine scarcity, many mechanisms of adaptation are readily activated inside and outside the thyroid gland. While thyrotropin (TSH) intervenes after severe ID to avoid hormonal deficit by stimulating both thyroid cell function and proliferation (Zimmermann, 2009), the thyroid gland continuously copes with moderate ID through several TSH-independent mechanisms, including the preferential synthesis of T3 over T4, the recycling of intracellular iodide, and the peripheral conversion of T4 into T3 (Pedraza et al., 2006; Kopp, 2008). In addition, thyrocytes constantly react to fluctuations in iodide availability by regulating their

Offprint requests to: Marie-Christine Many, Pole de Morphologie Expérimentale, Avnue Monier 52, box B1-52.04, Bussels, 1200, Belgium. e-mail: marie-christine.many@uclouvain.be

DOI: 10.14670/HH-11-727

Abbreviations. ID, Iodine Deficiency; HIF-1α, Hypoxia Inducible Factor 1α; ROS, Reactive oxygen species; NIS, Sodium Iodide Symporter; VEGF, Vascular Endothelial Growth Factor A; LID, Low Iodide Diet.

surrounding microvasculature (Gerard et al., 2008). This TSH-independent increase in blood flow is mediated, at least in part, by reactive oxygen species (ROS)-dependent stabilization of the α subunit of hypoxia inducible factor (HIF). This transcription factor up-regulates vascular endothelial growth factor (VEGF) expression, leading to an increase in VEGF protein secretion by the thyrocytes which results in a rise in the local blood flow, probably in order to adapt iodide delivery (Gerard et al., 2008, 2009). Although this microvascular activation is tightly controlled in healthy tissues, thyrocytes in a cancerous environment would lose the ability to fine-tune blood flow upon ID, thereby promoting tumor progression (Gerard et al., 2012).

Beside the thyroid gland, other organs express the iodide/sodium symporter (NIS), including salivary glands and the stomach, and might therefore be sensitive to ID. Both organs are characterized by active iodide uptake (MIRD, 1975; Bruno et al., 2004) probably to benefit from its antioxidant properties (Venturi and Venturi, 2007). Iodide is taken up at the basolateral membrane of the ductal cells in salivary glands and of mucin-secreting cells in the stomach. It is then secreted along its concentration gradient into the saliva and gastric fluids respectively (Brown-Grant, 1961; Josefsson et al., 2006). The physiological role for this iodide secretion is still uncertain, but evidence suggests that iodide may act as an antimicrobial agent in the saliva and gastric juice (Thomas et al., 1980; Geiszt et al., 2003; Portulano et al., 2014). It was hypothesized that salivary glands and the stomach could also be involved in systemic iodide recycling (Miller et al., 1975; Josefsson et al., 2002). As orally ingested iodide is normally absorbed by enterocytes to be partially cleared by the kidneys (Nicola et al., 2009), iodide taken up by salivary glands and the stomach could therefore escape from kidney clearance to be spared as a reserve potentially usable by the thyroid during ID periods.

Since salivary glands and the stomach are able to actively transport iodide, it is possible that they are also affected by ID. Consistently, in addition to the potential link between ID and dental carries (Venturi and Venturi, 2009), NIS expression was reported to be decreased in salivary glands during inflammation and tumor formation (La Perle et al., 2013). Accordingly, oxidized DNA and proteins are often found in oral cancers, possibly because of ID-associated oxidative stress (Bahar et al., 2007; Maier et al., 2007). Several studies also reported that ID is associated with stomach disorders. For instance, a higher rate of stomach cancers has been reported in iodine deficient areas in Poland, in China, and in Anatolia (Turkey) (Gulaboglu et al., 2005; Abnet et al., 2006; Golkowski et al., 2007). Moreover, patients with stomach cancer in Poland were more often diagnosed with goiter compared to the rest of the population when the country was still iodine-deficient. After iodine supplementation, both disorder rates decreased (Golkowski et al., 2007). At the molecular level, iodine concentration and NIS expression were reported to be lower in cancer tissues compared to the normal surrounding tissue (Gulaboglu et al., 2005; Altorjay et al., 2007).

While it seems that ID plays a role in different pathologies of diverse NIS-expressing organs, underlying mechanisms are still largely unknown. In this study, we investigated the potential effects of ID on the regulation of the local microvasculature in two NIS-expressing organs, salivary glands and stomach, and compared their biological response to ID to that of the thyroid.

Materials and methods

Animals and treatments

To induce ID, 8 week-old NMRI mice (strain 008, Harlan, Boxmeer, The Netherlands) were fed with a low-iodine diet (LID) (0.1 μg iodide/day; Animalabo, Brussels, Belgium) supplemented or not with 1% sodium perchlorate (a NIS inhibitor) in tap water for 1 to 10 days, or with a normal diet (0.4 mg iodide/kg, AO3, Scientific Animal Food and Engineering, Augy, France). ID was induced using the exact same protocol as in Gérard et al. (2008), where LID was combined with perchlorate (Bianco et al. 2014) in order to compare the effects of ID in the thyroid, the salivary glands and the stomach. Control animals received normal diet and tap water.

To inhibit VEGF-A, animals were injected intraperitoneally with a saline solution of bevacizumab (10 mg/kg; Roche, Welwyn Garden City, UK). Control animals were injected with an equimolar solution of irrelevant human IgGs (Sigma, St.-Louis, MO, USA). In both groups, animals were either fed a normal diet (controls) or LID supplemented with 1% sodium perchlorate in drinking water for 2 days.

Mice were housed and handled according to the Belgian regulation of Laboratory Animal Welfare. All *in vivo* experiments were performed with approval of UCL Comité d'Ethique pour l'Expérimentation Animale according to national and European animal care regulations.

Laser Doppler blood flow measurement and preparation of tissue samples

Mice were anesthetized with Ketamine (Anesketin, Eurovet, Belgium) and Xylasine (Rompun, Bayer HealthCare; Belgium) and placed on a heating pad (37°C). The skin was then incised and pulled aside to expose the submandibular glands, which are the most accessible salivary glands for blood flow measurements. Blood flow was measured using a Laser Doppler imager (Moor Instruments, Axminster, UK). Submandibular glands were identified and delineated based on anatomical images and blood flow was quantified based on corresponding colored histogram pixels. After measurements, mice were euthanized with an overdose

of pentothal (Abbott, Louvain, Belgium). Stomach and submandibular salivary glands were collected. Emptied stomach and a portion of salivary glands were fixed in paraformaldehyde (4% in phosphate-buffered saline [PBS]) for 36 hours and embedded in paraffin. Thick sections (5 μm) were used for immunohistochemistry and immunofluorescence. The remaining submandibular salivary glands were directly frozen in liquid nitrogen and used for protein analysis.

Western blots

Samples of salivary gland were homogenized into Laemmli buffer (10 ml Glycerol, 2 g SDS, 0.756 g Tris-hydroxymethylaminomethan, 0.19 g EDTA (5 mM) in a 100 ml distilled water solution) containing protease inhibitors (protease inhibitor cocktail tablets, Roche, Mannheim, Germany) and sonicated for 15 seconds. The protein content was measured using a BCA Protein assay kit (Pierce, Rockford, IL) according to manufacturer's protocol. Western blotting was performed as previously described (Gerard et al., 2012). Primary antibodies were incubated overnight at 4°C and secondary antibodies were incubated for one hour at room temperature (Table 1). Signal was detected using the Supersignal West Pico/Femto chemiluminescence kit from Thermo Scientific (Waltham, MA, USA). Western blots were scanned and the protein content of each sample was quantified by densitometry using NIH Scion ImageAnalysis Software (National Institutes of Health, Bethesda, MA). Protein levels were normalized to those of β-actin and GAPDH.

Immunohistochemistry

Immunohistochemistry was performed as previously described (Gerard et al., 2012). For VEGF-A detection, antigen retrieval was carried out: tissue sections were treated in a microwave oven in citrate buffer (0.01 M, pH 6) for one cycle of 3 min at 750 W, followed by 4 cycles of 3.5 min at 350 W. Then, sections were blocked in 1:50 non-immune goat serum (Vector Laboratories, Burlingame, CA, USA) in PBS/BSA 5% (albumin fraction V from bovine serum, VWR) for 30 min at room temperature. Antibodies, incubation times and dilutions are listed in Table 2. Primary antibodies were omitted in negative controls. Peroxidase activity was revealed with 3,3'-diaminobenzidine (DakoCytomation, Heverlee, Belgium). Sections were counterstained with Mayer's hematoxylin. Images were captured on an Axio scope A.1 microscope (Zeiss, Zaventem, Belgium) equipped with a DS-5Mc Color Digital Camera Head (Nikon, Amsterdam, The Netherlands).

Immunofluorescence

Sections from paraffin-embedded tissues were dewaxed in toluene and rehydrated in a series of graded alcohols to distilled water. Sections were washed three times in PBS-Triton X-100 (Sigma-Aldrich, St.-Louis, MO, USA) between each of the following steps. Slices were first quenched with $NaBH_4$ (10 mg/ml H_2O; sodium borohydride, Sigma-Aldrich). Antigen retrieval was performed as described above. After cooling down for 15 min, slices were blocked for 1 h in PBS/BSA 5%, and incubated at 4°C overnight with primary antibodies (VEGF-A, SC-152, Santa Cruz Biotechnology, 1/100; Ghrelin, SC-10368, Santa Cruz Biotechnology, 1/500) in PBS/BSA 2%. Primary antibodies were omitted in negative controls. Signals were revealed by 1-h incubation at room temperature in the dark with species-specific secondary antibodies conjugated to fluorophores (First: Alexa Fluor 488-conjugated donkey anti-goat, A-11055, Invitrogen, 1/300; second: Alexa Fluor 568-conjugated goat anti-rabbit, A11036, Invitrogen, 1/300) in PBS/BSA 1%. Nuclei were stained for 5 minutes with

Table 1. Western blot, primary and secondary antibody dilutions for HIF-1α, mNIS, β-actin, VEGFR1 and VEGFR2 proteins detection.

Protein	Primary Antibody	Primary antibody Dilution	Secondary antibody
HIF-1α	human/mouse/rat hif-1α, MAB-1536, R&D Systems	1:500	Biotinylated anti-Mouse, 1:200 (BA-9200, Labconsult)
NIS	NIS, SMC-391D, Stress Marq Biosciences Inc.	1:1000	Biotinylated anti-Mouse 1:200 (BA-9200, Labconsult)
β-Actin	β-actin, A5060, Sigma	1:5000	Goat anti-Rabbit Poly-HRP 1:5000(32260, Pierce)
VEGFR1	VEGF R1/Flt-1, AF471, R&D systems	1/1000	Biotinylated anti-Goat, 1:200 (BA-9500, Labconsult)
VEGFR2	VEGFR2/Flk-1, sc-6251, Santa Cruz Biotechnology	1/800	Biotinylated anti-Mouse 1:200 (BA-9200, Labconsult)

Table 2. Immunohistochemistry, primary and secondary antibody dilutions for VEGF-A and mNIS proteins detection.

Protein	Primary antibody	Primary antibody dilution and incubation time	Secondary antibody	Secondary antibody dilution and incubation time
VEGF-A	VEGF-A, SC-53462, Santa Cruz Biotechnology	-Salivary glands 1:75, o/n -Stomach 1:50, o/n	Goat anti-mouse poly-HRP, 32230, Pierce	1/50, 1 hour
NIS	NIS, a gift from Nancy Carrasco, Yale University School of Medicine, USA (Levy et al. 1997)	-Salivary glands 1:1500, 1 hour -Stomach 1:4000, 1 hour	Goat anti-rabbit poly-HRP, 32260, Pierce	1/50, 1 hour

4'-6'diamidino-2-phenylindole (DAPI, 1/10,000) and slides were mounted in Fluorescent Mounting Medium (Dako Cytomation). Images were captured on an AxioCam MRc5 fluorescence microscope using the Axio Vision 4.8 software (Zeiss).

Data analysis and statistics

All data are expressed as mean ± SEM. Experiments were conducted on groups of at least 3 mice and repeated independently 2 to 3 times (N=6-9), except for control experiment at days 20 and 30 (N=3). Statistical analysis was performed using one-way ANOVA with a Tukey-Kramer or a Dunnett multiple comparison or post hoc test or by using an unpaired Student *t* test when appropriate (GraphPad Instat, San Diego, CA, USA). $P<0.05$ was considered as statistically significant.

Results

Salivary glands

ID increases blood flow in salivary glands

Differences in basal blood flow in submandibular salivary glands were observed between male and female mice (Fig. 1). The results were therefore segregated by gender. A significant increase in blood flow was observed from day 1 to day 4 after ID induction in males and at day 2 in females (Fig. 1A). Blood flow then decreased to reach control levels at days 10 and 4, respectively. Although both male and female mice showed a transient rise in blood flow, the increase was proportionally stronger in males. A second experiment, with longer monitoring time showed no further changes in submandibular salivary glands up to 30 days after ID induction (Fig. 1B).

To discriminate between the LID-associated effects *versus* NIS inhibition by perchlorate and to eliminate the possibility that observed effects were due to an off-target effect of perchlorate, control experiments were carried out using either LID alone or perchlorate alone (data not shown). In males, LID treatment without perchlorate induced a significant transient increase in submandibular salivary gland blood flow at day 2, but no significant increase was seen in females at day 2, despite a trend. Conversely, perchlorate alone did not modulate blood flow significantly. Thus, salivary glands respond to ID by increasing local blood flow with additive effects between LID and perchlorate, at least in females.

ID increases HIF-1α and VEGF protein expression in salivary glands

In male mice, HIF-1α protein level was significantly increased at days 1 and 2 following ID induction, and decreased back to basal levels at days 4 and 10 (Fig. 2A). In females, HIF-1α protein expression increased at day 1 of ID to remain high up to day 10 (Fig. 2B).

Low expression of VEGF was detected using immunohistochemistry in duct cells of the submandibular salivary glands of both male (Fig. 3A) and female (Fig. 3B) control mice. From day 1 to day 4 of ID, VEGF immunostaining increased (Fig. 3C,D), to decrease thereafter and reach the control level at day 10 (Fig. 3E,F) in both male and female mice. Weak VEGF staining was also observed in the stroma between acini from day 2 to day 4 (Fig. 3C,D).

In order to prove the role of VEGF in ID-induced

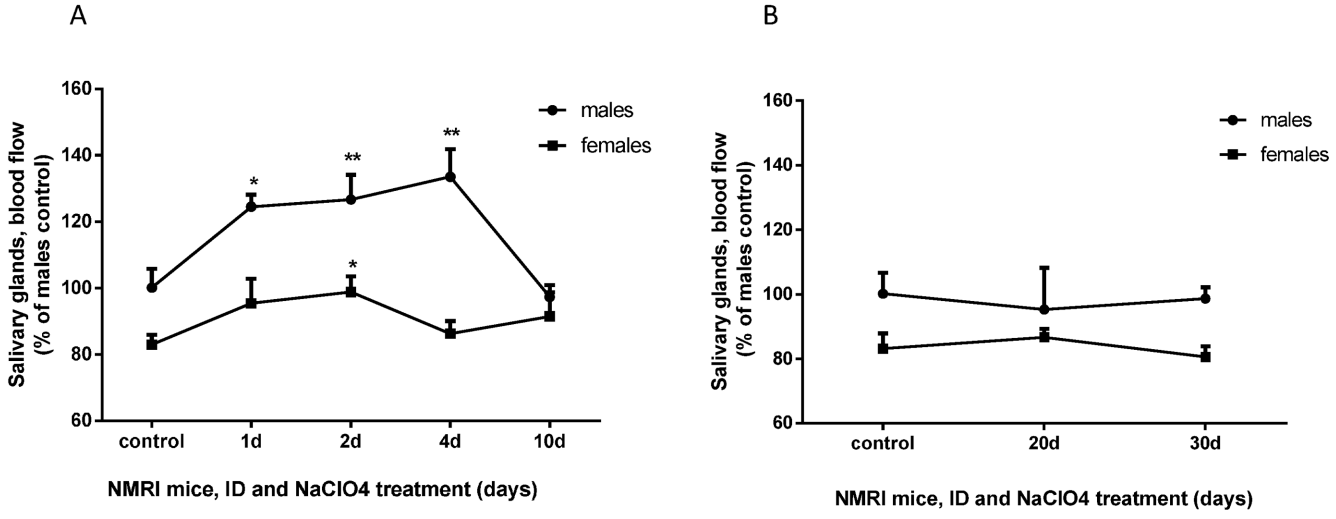

Fig. 1. NMRI mice salivary glands bloof blow after 0, 1, 2, 4 and 10 days of ID 3 (1b). **A**. Values are expressed as means ± SEM, N9. **B.** Values are expressed as means ± SEM, N=3. *p value <0.05, ** p value <0.01.

increase in salivary gland blood flow, the experiment was repeated with and without VEGF blocking antibody bevacizumab (Bock et al. 2007). In both male (Fig. 4A) and female (Fig. 4B) mice treated with irrelevant IgG, ID induced a significant rise in blood flow after 2 days of treatment, whereas blood flow was unchanged upon bevacizumab treatment. The blood flow was not affected by bevacizumab in control mice. Moreover, Western blot analyses of VEGF receptor 1 and 2 showed that their expression remained unchanged in mice treated with bevacizumab compared to control mice (data not shown) indicating that the expression of VEGF receptors 1 and 2 was not influenced by bevacizumab treatment. Thus, VEGF is at least partly responsible for the observed increase in blood flow in submandibular salivary glands during ID.

ID promotes NIS protein expression in salivary glands

Because salivary glands express the sodium/iodide symporter NIS (MIRD, 1975; Bruno et al., 2004), we looked at NIS expression in condition of ID to check whether decreased iodide bioavailability triggers NIS expression to optimize cellular iodine uptake. The immunohistochemical analysis showed that NIS expression in submandibular salivary glands is restricted to basolateral membranes of ductal cells (Fig. 5A,B). NIS expression increased in male and female mice over 2 days of ID (Fig. 5C,D), to decrease down to basal expression between days 4 and 10 (Fig. 5E,F). Changes were slightly more pronounced in males compared to females. These data were confirmed by Western blottings (data not shown).

Because NIS is the direct target of perchlorate, but perchlorate as a single treatment did not modify blood flow significantly in salivary glands, we compared NIS expression in animals treated with LID alone or perchlorate alone (data not shown). In males, LID and perchlorate used separately increased NIS expression at days 4 and 2, respectively. Similar data were obtained in female mice. NIS expression increase due to LID was delayed by 2 days compared to perchlorate treatment alone or LID/perchlorate co-treatment, confirming that perchlorate is used at a bioactive dose in our *in vivo* assays.

Stomach

ID stimulates VEGF expression in the stomach

Immunohistochemical detection showed no VEGF expression in mucin-secreting cells of control mice, but few capillaries underneath the epithelial layer were positively stained (Fig. 6A). Additionally, a few small cells located at the bottom of the tubular glands and surrounding the tubular glands showed positive cytoplasmic staining (Fig. 6B). After 1 day of ID, more

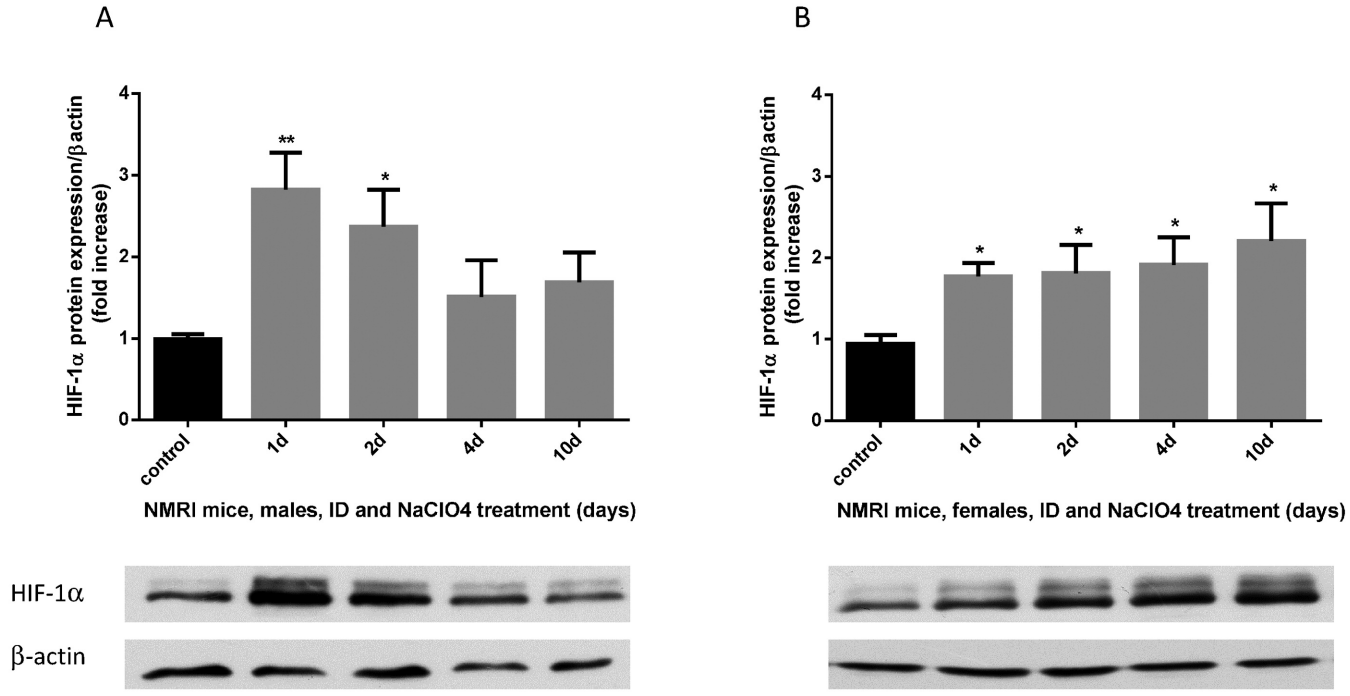

Fig. 2. HIF-1α protein expression in salivary glands of male **(A)** and female **(B)** NMRI mice after 0, 1, 2, 4 and 10 days of ID. Values are expressed as means ± SEM, N=9. *p value <0.05, **p value <0.01.

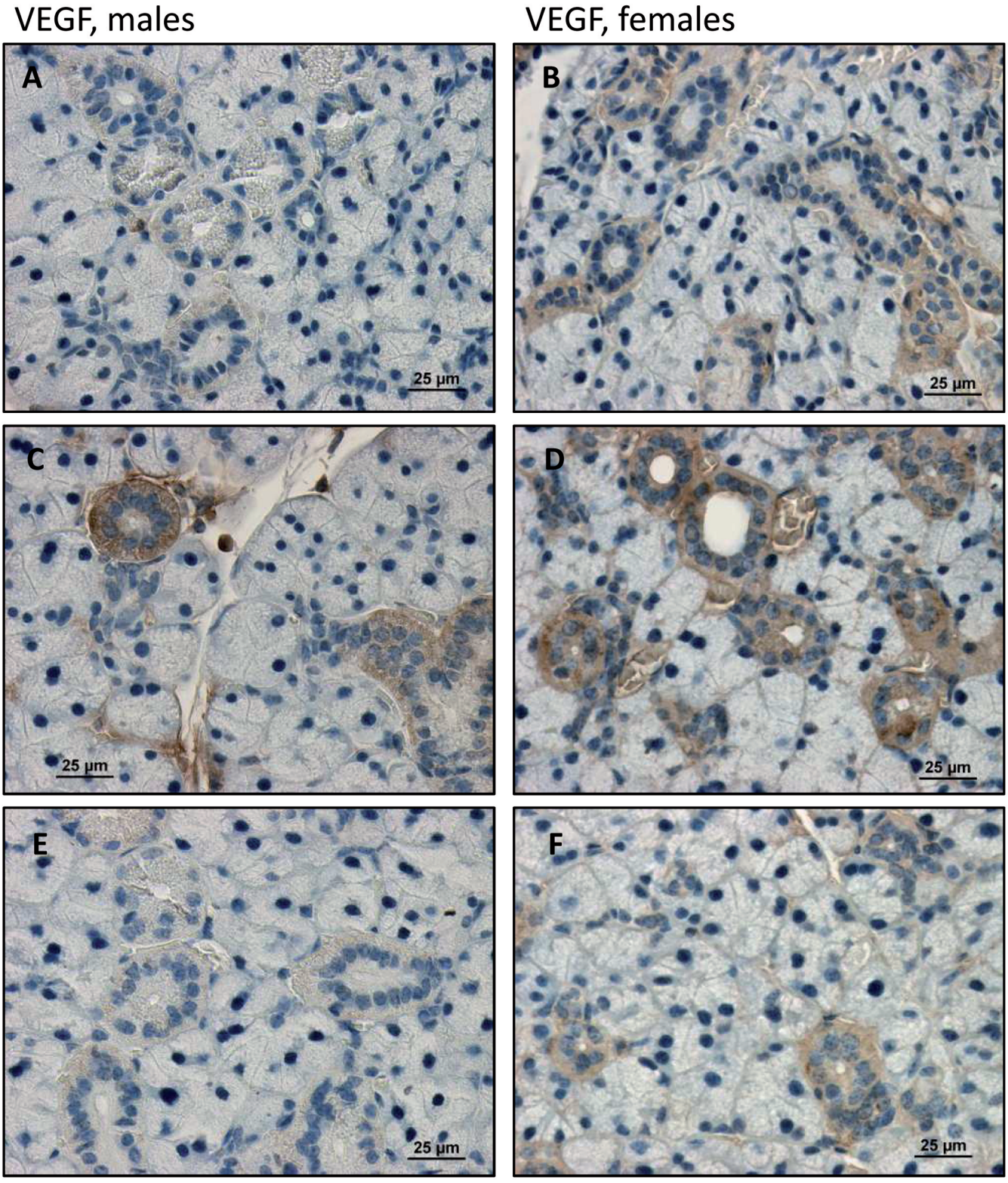

Fig. 3. Analysis of VEG expression by immunohiostochemistry in salivary glands (serous acini and ducts): **A, B.** Control. **C, D.** ID 2 day. **E, F.** ID 10 days.

capillaries under the mucin-secreting epithelium and more cells in tubular glands were stained (Fig. 6D,E). After 2 days of ID, increased VEGF staining was also observed inside the cytoplasm of most mucin-secreting cells, which are NIS-expressing cells (Fig. 6G). The increase in VEGF expression lasted until day 4 of ID, after which it decreased up to day 10 (Fig. 6J,K). Compared to control mice, VEGF signal at day 10 of ID was slightly stronger in the vessels underneath mucin-secreting cells, but not in the small cells located in the tubular glands. Additional experiments showed that LID and perchlorate as separate treatments did increase VEGF expression (data not shown).

The cells expressing VEGF at the bottom of the tubular gland during ID were localized around the tubular glands and their size was smaller than that of parietal cells. As these characteristics are compatible with gastric endocrine cells, we performed a double immunofluorescence staining for both VEGF and a well expressed gastric hormone, ghrelin (Fig. 7). In control mice, ghrelin-expressing cells (G-cells) did not express VEGF (Fig. 7A-C), whereas the vast majority of G-cells were double stained with VEGF in ID mice (Fig. 7D-F). Of note, a few cells expressed VEGF, but not ghrelin, in ID mice.

ID induces a slight increase followed by a decrease in NIS expression

NIS protein expression was also looked at in the stomach. In basal conditions, a positive immunohistochemical staining for NIS was visible only at the basolateral membrane of mucin-secreting cells (Fig. 6C), but not in parietal cells. ID induced a weak increase in NIS staining at day 1 (Fig. 6F), which was followed by a strong decrease from day 2 to 10 (Fig. 6I, L). LID and perchlorate as separate agents both induced a decrease in NIS expression on day 2 (data not shown), confirming that NIS expression is controlled by ID rather than by any off-target effect of perchlorate. Thus, in contrast to the salivary glands, ID induced only a slight increase which was followed by a strong decrease in NIS expression in the stomach.

Discussion

While several epidemiological studies have associated ID to disorders in salivary glands and in the stomach (Gulaboglu et al., 2005; Abnet et al., 2006; Golkowski et al., 2007; Venturi and Venturi, 2009; La Perle et al., 2013), few studies have addressed the molecular effects of ID in these organs. Here, we report that, as already described in the thyroid (Gerard et al. 2008), salivary glands and the stomach respond to ID by inducing a microvascular response.

A striking similarity between these three NIS-expressing tissues is the rapid ID-induced increase in VEGF expression and in the local blood flow (at least in salivary glands and thyroid). In the thyroid, the microvascular response that occurs in response to ID to

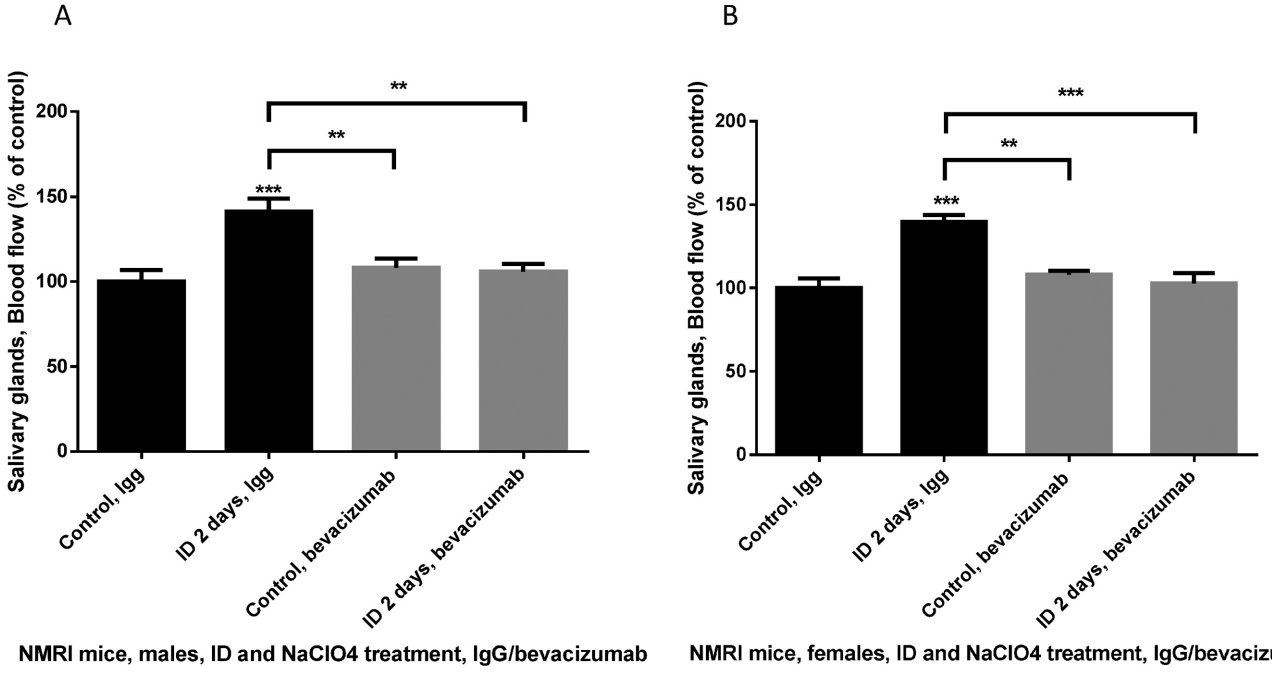

Fig. 4. Salivary gland blood flow after 0 or 2 days of ID in male **(A)** and female (**B)** mice pre-injected with bevacizumban or IgG in order to assess VEGF involvement in blood flow levels. Values are expressed as means ± SEM, N=6 * p value <0.01, *** p value <0.001.

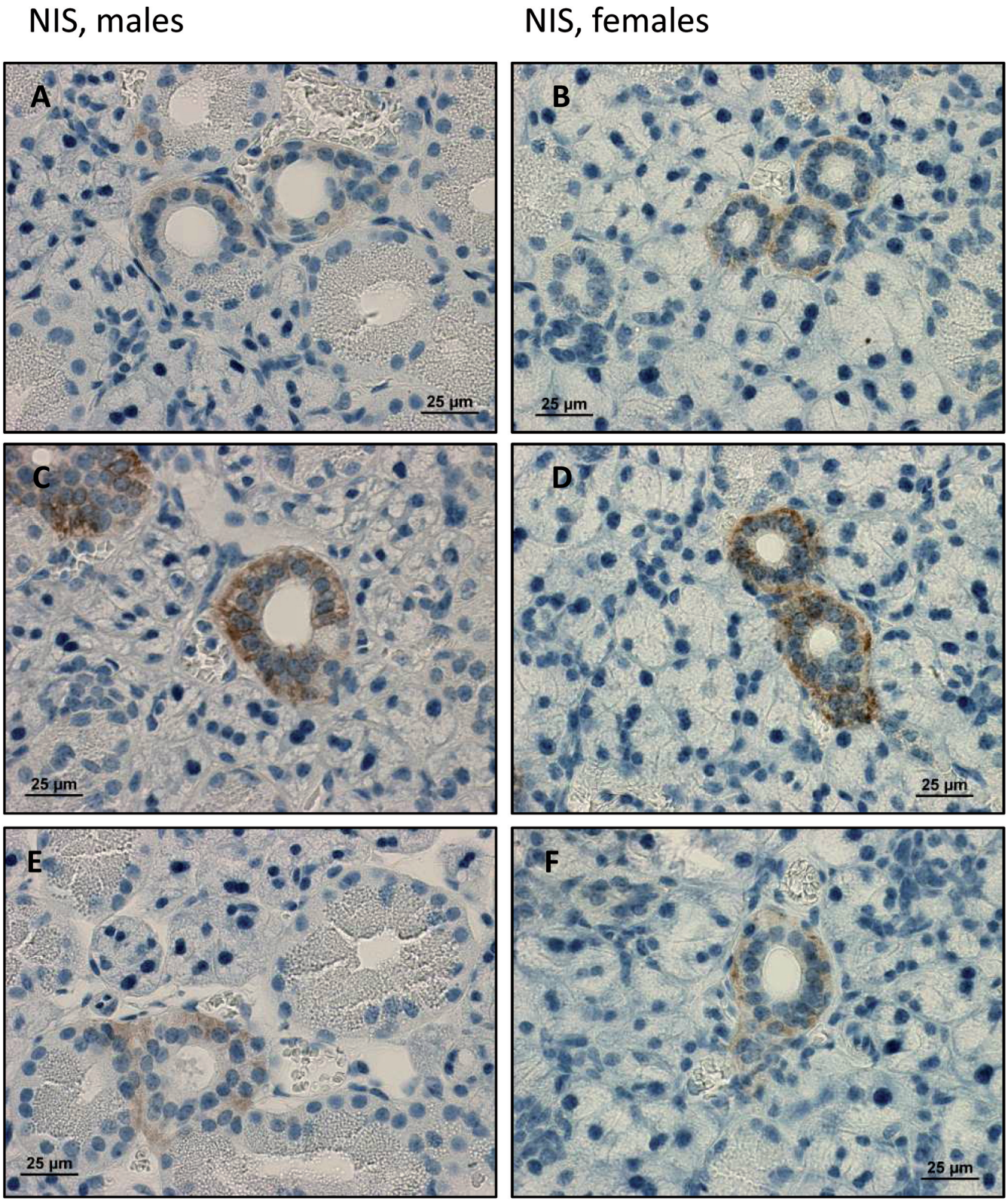

Fig. 5. Analysis of NIS expression by immunohistochemistry in salivary glands (serous acini and ducts), **A, B.** Control. **C, D.** ID 2 day. **E, F.** ID 10 days.

improve the local supply of iodide is biphasic (Gerard et al., 2008). An early transient TSH-independent response occurs already at day 1 of ID with thyrocytes releasing VEGF which directly acts on adjacent capillaries. A second delayed phase then takes place when ID-induced impaired thyroid hormone synthesis triggers TSH production from the pituitary gland which further stimulates VEGF secretion from thyrocytes. In salivary glands and in the stomach, a rapid, but only transient, ID-induced increase in VEGF expression was observed

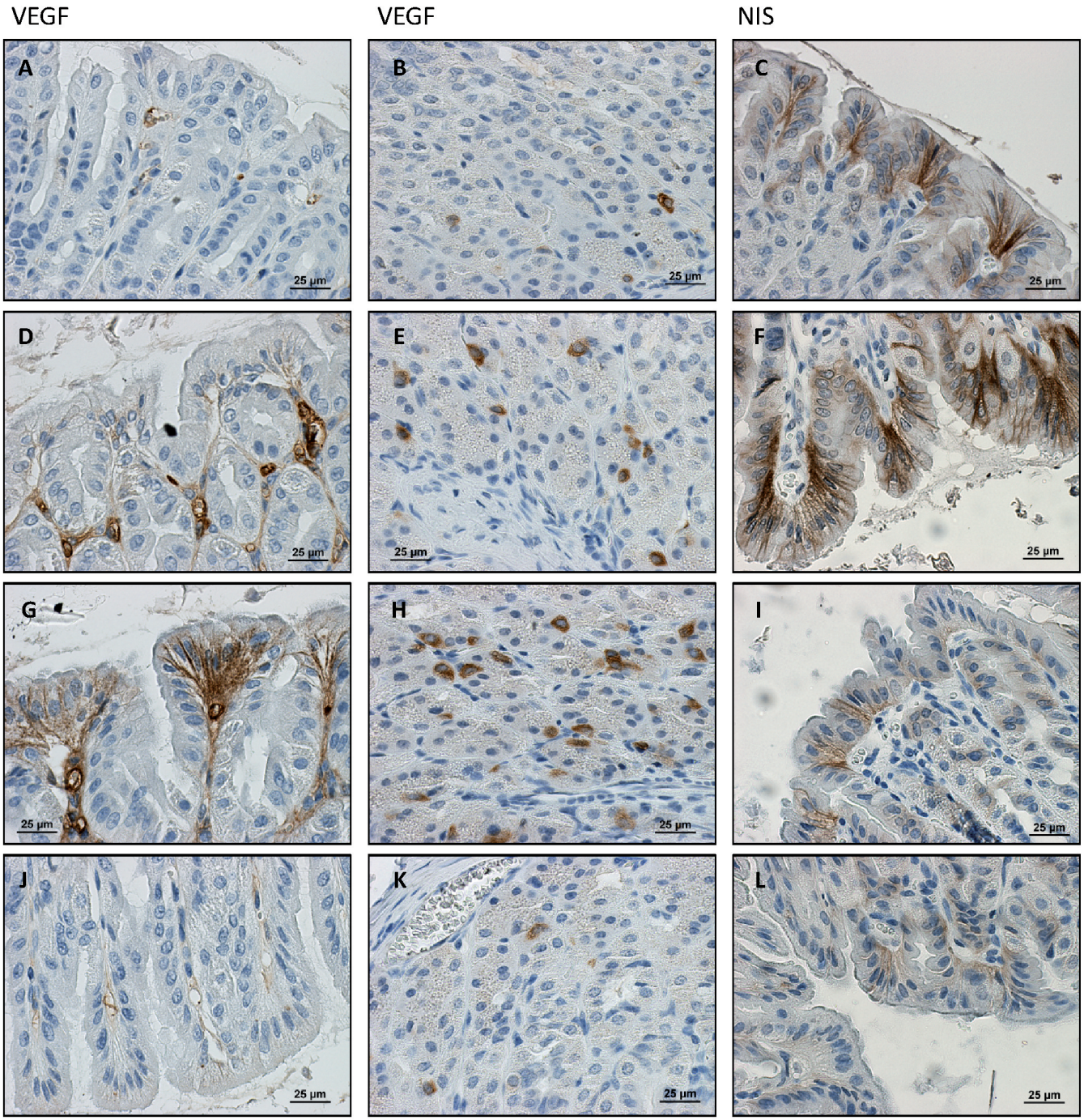

FIG. 6. Analysis of VEGF and NIS expression by immunohistochemistry in stomach. **A, B.** VEG, Control. **C.** NIS, control. **D, E.** VEG, ID 1 day. **F.** NIS, ID 1 day. **G, H.** VEGF, ID, 2 days. **I.** NIS, ID 2 days. **J, K.** VEGF, ID 10 days. **L.** NIS, ID 10 days. x 40

and it was associated with an increase in blood flow in the salivary glands. This may also occur in the stomach but this hypothesis cannot be verified because the gastric mucosa is not accessible for Laser Doppler measurements due to the presence of muscles. We therefore focused on VEGF as ID response effector and documented increased VEGF staining in small blood vessels close to mucin secreting epithelial cells, which are known to express NIS (Altorjay et al. 2007), while only few of them were positively stained in control mice, suggesting endothelial activation by VEGF during ID in the stomach. In contrast with the thyroid, the delayed TSH-dependent phase was not observed, which is in accordance with the fact that salivary glands and the stomach are not sensitive to TSH signaling (Viglietto et al., 1997; Josefsson et al., 2006; Gerard et al., 2008; Portulano et al., 2014).

In their early transient response to ID, the thyroid and salivary glands share a similar molecular pathway. In both organs ((Gerard et al., 2008, 2009) and this study), increased blood flow is preceded by an increased expression of HIF-1 transcription factor subunit α. This subunit is known to bind to HIF-1β to form active HIF-1 and to stimulate the expression of target genes including VEGF. Accordingly, ID increases VEGF production by thyrocytes (Gerard et al., 2008, 2009), and by ductal cells in serous acini of the salivary glands. The active contribution of VEGF to the increased microvascular perfusion was clearly demonstrated in salivary glands where bevacizumab inhibited ID effects. This does not rule out the potential involvement of other pro-angiogenic factors such as FGF2 in response to ID, as already reported in the thyroid (Gerard et al., 2008, 2009). Like thyrocytes and ductal cells of the salivary glands, mucin-secreting epithelial cells in the stomach are NIS expressing cells (Jhiang et al., 1998; Altorjay et al., 2007) and also responded to ID by increasing VEGF production. It is therefore reasonable to postulate that, as already reported in the thyroid gland, NIS-expressing cells in salivary glands and in the stomach are sensitive to ID. In addition to mucin-secreting cells, ghrelin positive endocrine cells also overexpressed VEGF when

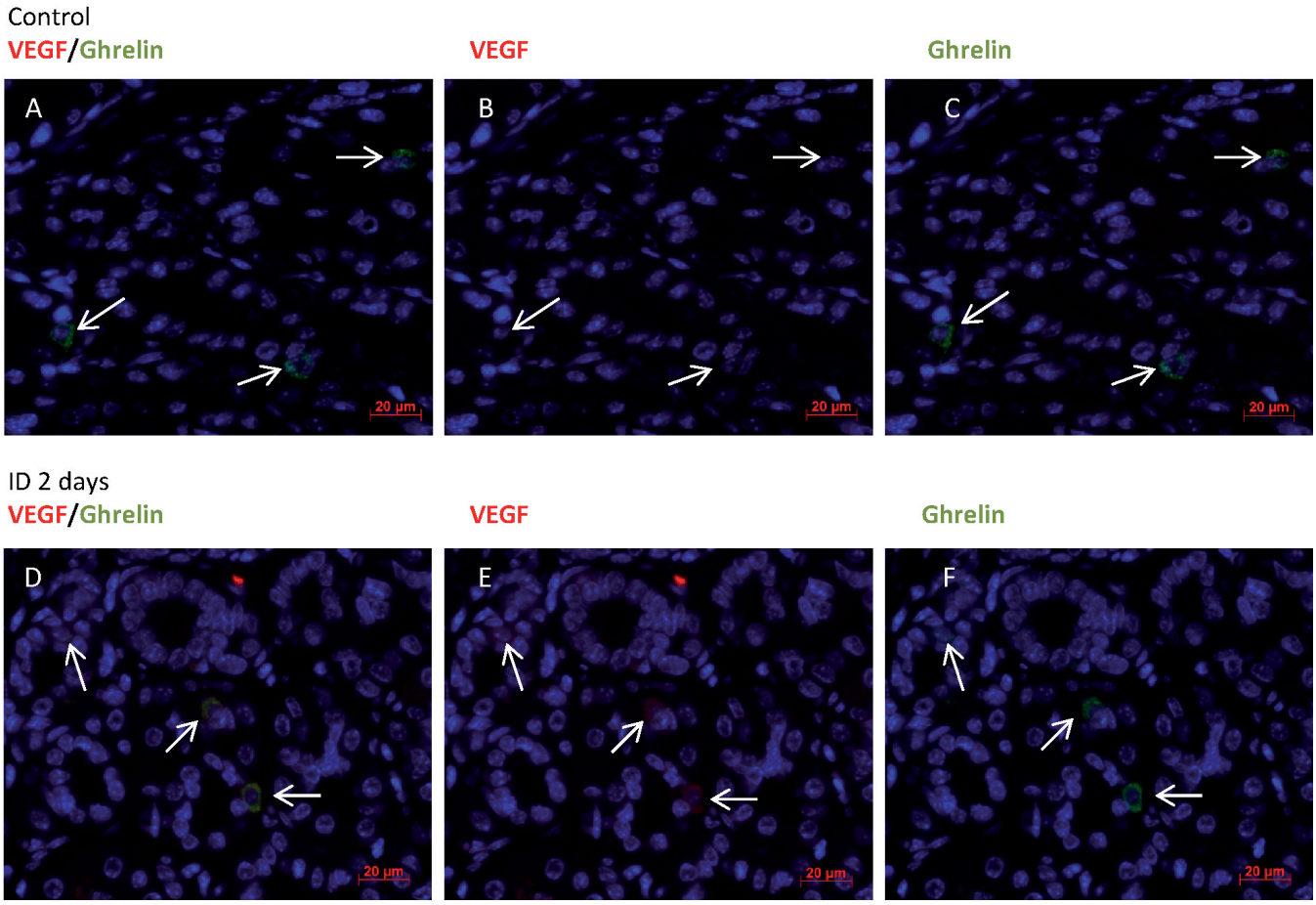

Fig. 7. Analysis of VEGF and ghrelin expression by immunofluorescence in stomach, **A-C.** Control. **D-F.** ID, 2 days. Red: VEGF. Green: Ghrelin, **A, D.** VEG/Ghrelin double staining. **B, E.** VEGF staining. **C, F.** Ghrelin staining. x 40

exposed to ID, even though NIS expression was not reported in gastric endocrine cells to our knowledge (Kotani et al., 1998; Vayre et al., 1999; Altorjay et al., 2007). Moreover, a few cells located at the bottom end of the tubular glands did overexpress VEGF but not ghrelin. Based on their localization and because they were of the same size as ghrelin-expressing cells, it is reasonable to propose that they correspond to another type of gastric endocrine cells. While it is also possible that among those cells, a few are mast cells, which are known to secrete VEGF (Ribatti and Crivellato, 2012), mast cells were too few in the stroma between the glands (unpublished results), to account for the population of cells expressing VEGF but not ghrelin. We cannot yet interpret the physiological relevance of this observation that obviously requires further investigations.

It is proposed that iodide exerts antioxidative effects, which may explain the early release of ROS and nitric oxide (NO) in response to ID in the thyroid gland. In this organ, ROS and NO can stabilize HIF-1α and activate HIF-1 during ID in thyroid cells (Gerard et al., 2008, 2009; Craps et al., 2015). Thus, it is likely that redox stress initiates the HIF-1-VEGF response to ID in NIS-expressing cells, which will be addressed experimentally in further investigation. Similarly, it remains to be determined if the changes in NIS expression induced by ID in salivary glands and in stomach originates from a redox imbalance. NIS is not a HIF-1 target gene (Yeom et al., 2008), but its expression is sensitive to redox changes (Serrano-Nascimento et al., 2014). However, NIS expression is transiently increased in salivary glands and only slightly increased, then decreased in the stomach. Its regulation is thus influenced by iodide supply in both organs but may depend on different molecular pathways.

In the thyroid, salivary glands and stomach, functional consequences of the molecular responses to ID could represent strategies aimed at improving iodide supply. By increasing local perfusion, NIS-expressing cells would promote local iodide supply from blood. In salivary glands, a second strategy would be to increase NIS expression in duct cells, in order to optimize iodide uptake. Accordingly, cellular responses were maximal when both iodine ingestion (LID) and NIS activity (perchlorate) were impaired. Although the role of iodide in salivary glands and the stomach has not yet been totally clarified, three possibilities have been evoked: an antioxidant, a bactericidal and a recycling function (Thomas et al., 1980; Josefsson et al., 2002; Geiszt et al., 2003; Venturi and Venturi, 2007, 2009; Portulano et al., 2014). Thus, when facing ID, salivary glands and the stomach might try to optimize iodide intake to benefit from its antioxidant and bactericidal properties. It is also possible that by recycling iodide into the blood circulation via the enteroenteric circulation, this would reduce its clearance through the kidneys, as suggested by Miller et al. (1975) and Josefsson et al. (2002), thereby optimizing iodide supply to the thyroid gland. This mechanism of iodide sparing should therefore be considered in addition to those activated by the thyroid, including the improved local supply of iodide through increased microvascular flow, the preferential synthesis of T3 over T4 and the internal recycling of unused mono- and di-iodotyrosines (Pedraza et al., 2006; Kopp, 2008). Further arguments are required to strengthen the validity of this hypothesis.

It is worth mentioning that a gender difference in the response to ID was observed. Gender-associated differences in salivary gland functions have already been reported in several studies (Ferguson and Stephen, 1972; Lazarus et al., 1974), but our observation that basal blood flow is higher in the submandibular salivary glands of male compared to female mice is, to our knowledge, unprecedented. In addition, male salivary glands showed a stronger response to ID. LID alone was sufficient to significantly enhance salivary gland blood flow while perchlorate alone had no significant effect in males. In females, maximal effects required combined treatment. Accordingly, while NIS is known to be expressed only in salivary ducts and iodide uptake has been observed in duct cells in both males and females (Ferguson and Stephen, 1972; Jhiang et al., 1998), a higher iodide concentration was reported in male compared to female ducts (Lazarus et al., 1974). Thus, the difference that we observed in the amplitude of salivary glands response to ID between males and females follows the same trend as the capacity of the glands to concentrate iodide. However, while a concordance was observed between changes in HIF-1α and VEGF levels and blood flow in males, HIF-1α levels remained elevated in females even after the end of the microvascular reaction, suggesting the existence of other molecular pathways that regulate ID-induced blood flow in a gender-specific manner.

In conclusion, our study reports that ID induces microvascular responses in salivary glands and in the stomach similar to those previously observed in the thyroid. It is reasonable to postulate that this microvascular activation that occurs in response to ID in these two NIS-expressing tissues contributes to optimize as much as possible the local delivery of iodide in periods of iodide deprivation.

Acknowledgements. This study has been supported by grants from the Fonds National de la Recherche Scientifique (F.R.S.-FNRS) (project J.0112.13), the Belgian Federal Agency for Nuclear Control (AFCN-FANC) and FP7/2007-2013 ERC Independent Researcher Starting Grant 243188 TUMETABO to PS. PS is a Research Associate of the F.R.S.-FNRS. The authors thank Benoît Lengelé, head of the pole of Morphologie Expérimentale, for his support. Authors also thank Nancy Carrasco (Yale University School of Medicine, CT, USA) and Françoise Miot (ULB, Brussels, Belgium) for the kind gift of anti-NIS antibody, Christine de Ville de Goyet (UCL) and Luminita Nae (Institut Paul Lambin, Brussels) for expert technical support, and Quentin Binet (UCL) for technical assistance.

Disclosure statement. The authors declare that no conflict of interest exists.

References

Abnet C.C., Fan J.H., Kamangar F., Sun X.D., Taylor P.R., Ren J.S., Mark S.D., Zhao P., Fraumeni J.F. Jr, Qiao Y.L. and Dawsey S.M. (2006). Self-reported goiter is associated with a significantly increased risk of gastric noncardia adenocarcinoma in a large population-based Chinese cohort. Int. J. Cancer 119, 1508-1510.

Altorjay A., Dohan O., Szilagyi A., Paroder M., Wapnir I.L. and Carrasco N. (2007). Expression of the Na+/I- symporter (NIS) is markedly decreased or absent in gastric cancer and intestinal metaplastic mucosa of Barrett esophagus. BMC Cancer 7, 5.

Andersson M. and Zimmermann M. (2012). Global iodine nutrition: a remarkable leap forward in the past decade. IDD newsletter 40.

Bahar G., Feinmesser R., Shpitzer T., Popovtzer A. and Nagler R.M. (2007). Salivary analysis in oral cancer patients: DNA and protein oxidation, reactive nitrogen species, and antioxidant profile. Cancer 109, 54-59.

Bianco A.C., Anderson G., Forrest D., Galton V.A., Gereben B., Kim B.W., Kopp P.A., Liao X.H., Obregon M.J., Peeters R.P., Refetoff S., Sharlin D.S., Simonides W.S., Weiss R.E. and Williams G.R. (2014). American Thyroid Association Guide to investigating thyroid hormone economy and action in rodent and cell models. Thyroid 24, 88-168.

Bock F., Onderka J., Dietrich T., Bachmann B., Kruse F.E., Paschke M., Zahn G. and Cursiefen C. (2007). Bevacizumab as a potent inhibitor of inflammatory corneal angiogenesis and lymphangiogenesis. Invest. Ophthalmol. Vis. Sci. 48, 2545-2552.

Brown-Grant K. (1961). Extrathyroidal iodide concentrating mechanisms. Physiol. Rev. 41, 189-213.

Bruno R., Giannasio P., Ronga G., Baudin E., Travagli J.P., Russo D., Filetti S. and Schlumberger M. (2004). Sodium iodide symporter expression and radioiodine distribution in extrathyroidal tissues. J. Endocrinol. Invest. 27, 1010-1014.

Craps J., Wilvers C., Joris V., De Jongh B., Vanderstraeten J., Lobysheva I., Balligand J.L., Sonveaux P., Gilon P., Many M.C., Gerard A.C. and Colin I.M. (2015). Involvement of nitric oxide in iodine deficiency-induced microvascular remodeling in the thyroid gland: role of nitric oxide synthase 3 and ryanodine receptors. Endocrinology 156, 707-720.

Ferguson M.M. and Stephen K.W. (1972). Sex differences in the autoradiographic pattern of (^{125}I)iodide uptake in mouse submandibular salivary gland. Arch. Oral Biol. 17, 1117-1119.

Geiszt M., Witta J., Baffi J., Lekstrom K. and Leto T.L. (2003). Dual oxidases represent novel hydrogen peroxide sources supporting mucosal surface host defense. FASEB J. 17, 1502-1504.

Gerard A.C., Humblet K., Wilvers C., Poncin S., Derradji H., de Ville de G.C., Abou-el-Ardat K., Baatout S., Sonveaux P., Denef J.F. and Colin I.M. (2012). Iodine-deficiency-induced long lasting angiogenic reaction in thyroid cancers occurs via a vascular endothelial growth factor-hypoxia inducible factor-1-dependent, but not a reactive oxygen species-dependent, pathway. Thyroid 22, 699-708.

Gerard A.C., Poncin S., Audinot J.N., Denef J.F. and Colin I.M. (2009). Iodide deficiency-induced angiogenic stimulus in the thyroid occurs via HIF- and ROS-dependent VEGF-A secretion from thyrocytes. Am. J. Physiol. Endocrinol. Metab. 296, E1414-E1422.

Gerard A.C., Poncin S., Caetano B., Sonveaux P., Audinot J.N., Feron O., Colin I.M. and Soncin F. (2008). Iodine deficiency induces a thyroid stimulating hormone-independent early phase of microvascular reshaping in the thyroid. Am. J. Pathol. 172, 748-760.

Golkowski F., Szybinski Z., Rachtan J., Sokolowski A., Buziak-Bereza M., Trofimiuk M., Hubalewska-Dydejczyk A., Przybylik-Mazurek E. and Huszno B. (2007). Iodine prophylaxis--the protective factor against stomach cancer in iodine deficient areas. Eur. J. Nutr. 46, 251-256.

Gulaboglu M., Yildiz L., Celebi F., Gul M. and Peker K. (2005). Comparison of iodine contents in gastric cancer and surrounding normal tissues. Clin. Chem. Lab. Med. 43, 581-584.

Jhiang S.M., Cho J.Y., Ryu K.Y., De Young B.R., Smanik P.A., McGaughy V.R., Fischer A.H. and Mazzaferri E.L. (1998). An immunohistochemical study of Na+/I- symporter in human thyroid tissues and salivary gland tissues. Endocrinology 139, 4416-4419.

Josefsson M., Evilevitch L., Westrom B., Grunditz T. and Ekblad E. (2006). Sodium-iodide symporter mediates iodide secretion in rat gastric mucosa *in vitro*. Exp. Biol. Med.(Maywood.) 231, 277-281.

Josefsson M., Grunditz T., Ohlsson T. and Ekblad E. (2002). Sodium/iodide-symporter: distribution in different mammals and role in entero-thyroid circulation of iodide. Acta Physiol. Scand. 175, 129-137.

Kopp P.A. (2008). Reduce, recycle, reuse--iodotyrosine deiodinase in thyroid iodide metabolism. N. Engl. J. Med. 358, 1856-1859.

Kotani T., Ogata Y., Yamamoto I., Aratake Y., Kawano J.I., Suganuma T. and Ohtaki S (1998). Characterization of gastric Na+/I- symporter of the rat. Clin. Immunol. Immunopathol. 89, 271-278.

La Perle K.M., Kim D.C., Hall N.C., Bobbey A., Shen D.H., Nagy R.S., Wakely P.E. Jr, Lehman A., Jarjoura D. and Jhiang S.M. (2013). Modulation of sodium/iodide symporter expression in the salivary gland. Thyroid 23, 1029-1036.

Lazarus J.H., Harden R.M. and Robertson J.W. (1974). Quantitative studies of the inhibitory effect of perchlorate on the concentration of 36C1O minus 4 125I minus and 99mTcO minus 4 in salivary glands of male and female mice. Arch. Oral Biol. 19, 493-498.

Levy O., Dai G., Riedel C., Ginter C.S., Paul E.M., Lebowitz A.N. and Carrasco N. (1997). Characterization of the thyroid Na+/I- symporter with an anti-COOH terminus antibody. Proc. Natl. Acad. Sci. USA 94, 5568-5573.

Maier J., van S.H., van O.C., Paschke R., Weiss R.E. and Krohn K. (2007). Iodine deficiency activates antioxidant genes and causes DNA damage in the thyroid gland of rats and mice. Biochim. Biophys. Acta 1773, 990-999.

Miller J.K., Swanson E.W. and Spalding G.E. (1975). Iodine absorption, excretion, recycling, and tissue distribution in the dairy cow. J. Dairy Sci. 58, 1578-1593.

MIRD (1975). Summary of current radiation dose estimates to humans from ^{123}I, ^{124}I, ^{125}I, ^{126}I, ^{130}I, ^{131}I, and ^{132}I as sodium iodide. J. Nucl. Med. 16, 857-860.

Nicola J.P., Basquin C., Portulano C., Reyna-Neyra A., Paroder M. and Carrasco N. (2009). The Na+/I- symporter mediates active iodide uptake in the intestine. Am. J. Physiol. Cell Physiol. 296, C654-C662.

Pearce E.N., Andersson M. and Zimmermann M.B. (2013). Global iodine nutrition: Where do we stand in 2013? Thyroid 23, 523-528.

Pedraza P.E., Obregon M.J., Escobar-Morreale H.F., del Rey F.E. and de Escobar G.M. (2006). Mechanisms of adaptation to iodine deficiency in rats: thyroid status is tissue specific. Its relevance for man. Endocrinology 147, 2098-2108.

Portulano C., Paroder-Belenitsky M. and Carrasco N. (2014). The Na+/I-symporter (NIS): mechanism and medical impact. Endocr. Rev. 35,

106-149.
Ribatti D. and Crivellato E. (2012). Mast cells, angiogenesis, and tumour growth. Biochim. Biophys. Acta (BBA). 1822, 2-8.
Serrano-Nascimento C., da Silva T.S., Nicola J.P., Nachbar R.T., Masini-Repiso A.M. and Nunes M.T. (2014). The acute inhibitory effect of iodide excess on sodium/iodide symporter expression and activity involves the PI3K/Akt signaling pathway. Endocrinology 155, 1145-1156.
Thomas E.L., Bates K.P. and Jefferson M.M. (1980). Hypothiocyanite ion: detection of the antimicrobial agent in human saliva. J. Dent. Res. 59, 1466-1472.
Vayre L., Sabourin J.C., Caillou B., Ducreux M., Schlumberger M. and Bidart J.M. (1999). Immunohistochemical analysis of Na+/I-symporter distribution in human extra-thyroidal tissues. Eur. J. Endocrinol. 141, 382-386.
Venturi S. and Venturi M. (2007). Evolution of dietary antioxidant defences. Eur. Epi-Marker 11, 1-12.
Venturi S. and Venturi M. (2009). Iodine in evolution of salivary glands and in oral health. Nutr. Health 20, 119-134.
Viglietto G., Romano A., Manzo G., Chiappetta G., Paoletti I., Califano D., Galati M.G., Mauriello V., Bruni P., Lago C.T., Fusco A. and Persico M.G. (1997). Upregulation of the angiogenic factors PlGF, VEGF and their receptors (Flt-1, Flk-1/KDR) by TSH in cultured thyrocytes and in the thyroid gland of thiouracil-fed rats suggest a TSH-dependent paracrine mechanism for goiter hyper-vascularization. Oncogene 15, 2687-2698.
WHO (2015). http://www.who.int/vmnis/database/iodine/iodine_data_status_summary/en/
Yeom C.J., Chung J.K., Kang J.H., Jeon Y.H., Kim K.I., Jin Y.N., Lee Y.M., Jeong J.M. and Lee D.S. (2008). Visualization of hypoxia-inducible factor-1 transcriptional activation in C6 glioma using luciferase and sodium iodide symporter genes. J. Nucl. Med. 49, 1489-1497.
Zimmermann M.B. (2009). Iodine deficiency. Endocr. Rev. 30, 376-408.

Accepted February 3, 2016